

# **V International Scientific and Technical Conference Actual Issues of Power Supply Systems**

---

## **Improvement of the magnetic field measurement device for an asynchronous motor and implementation of diagnostics**

AIPCP25-CF-ICAIPSS2025-00548 | Article

PDF auto-generated using **ReView**



# Improvement of the magnetic field measurement device for an asynchronous motor, and implementation of diagnostics

Olimjon Toirov<sup>1</sup>, Jasurbek Nizamov<sup>2</sup>, Fozil Sharopov<sup>3,a)</sup>, Xumoyun Xaydarov<sup>2</sup>, Shuxratbek Mannobboyev<sup>2</sup>, Dilnoza Jumaeva<sup>4</sup>

<sup>1</sup>*Tashkent State Technical University named after Islam Karimov, Tashkent, Uzbekistan*

<sup>2</sup>*Andijan state technical institute, Andijan, Uzbekistan*

<sup>3</sup>*Institute of Energy Problems of the Academy of Sciences of the Republic of Uzbekistan, Tashkent, Uzbekistan*

<sup>4</sup>*Institute of General and Inorganic Chemistry of the Academy of Sciences of Uzbekistan, Tashkent, Uzbekistan*

<sup>a)</sup> Corresponding author: [sharopovfozilqobilovich@gmail.com](mailto:sharopovfozilqobilovich@gmail.com)

**Abstract.** This article presents an improved magnetic field measurement system designed for fault detection in asynchronous electric motors. A high-sensitivity Hall-effect sensor array was developed and positioned along both the air gap and external regions of the motor to detect magnetic flux variations under different operating conditions. A mathematical model based on the dq-coordinate system and finite element method (FEM) was formulated, accounting for nonlinear factors such as magnetic saturation and slot effects. Simulation results showed strong correlation with experimental data, with average deviations of 4.37% in the air gap field and 6.85% in the external stray magnetic field. The proposed system effectively detects rotor bar fractures, stator winding short circuits, and bearing faults by analyzing changes in flux amplitude and phase angle. Furthermore, a simplified external measurement device was introduced for real-time, non-invasive diagnostics. This approach offers a cost-effective and reliable solution for monitoring motor health in industrial environments and supports the development of predictive maintenance strategies.

## INTRODUCTION

Induction motors play a vital role in modern industrial applications due to their robustness, simplicity, and cost efficiency. However, their reliable operation is often compromised by internal faults such as broken rotor bars, stator winding short circuits, and bearing wear, which can cause performance degradation and unexpected downtime [1]. Traditional diagnostic methods, including motor current signature analysis, vibration monitoring, and thermal measurements, frequently face challenges in detecting early-stage faults, especially under varying load conditions. Consequently, investigating the internal magnetic field variations within the motor has emerged as an effective approach for fault detection. Changes in the magnetic field directly reflect electromagnetic and mechanical anomalies occurring inside the machine. This study presents the development of an enhanced magnetic field measurement system utilizing high-sensitivity Hall-effect sensors to capture both internal air-gap and external stray magnetic fields in real time [2]. Additionally, a mathematical model based on the *dq*-coordinate transformation was formulated to simulate healthy and faulty motor states. Experimental validation confirms strong agreement between the model predictions and measured data, demonstrating the proposed method's reliability and potential for early fault diagnosis in induction motors.

## EXPERIMENTAL RESEARCH

This chapter presents the electromagnetic processes in asynchronous machines, the mathematical model and calculation algorithm of the internal (air gap) magnetic field, and the mathematical model and calculation algorithm of the external magnetic field of an asynchronous machine [3]. The magnetic field generated in an electric machine is not uniformly distributed; therefore, its magnetic effect depends on the density of the magnetic flux lines. The

appearance of the magnetic field depends on the load, voltage, operating mode, and the geometric shape of the magnetic system. Using the orthogonal model, the total magnetic flux of the asynchronous machine is calculated. The  $dq$  system is used to study the instantaneous values of the stator and rotor [4]. By transforming the magnetic flux variation equation from the (a, b, c) coordinate system to the ( $\alpha$ ,  $\beta$ , 0) polar coordinate system, the following operations are performed to obtain the stator and rotor equilibrium equations. Using the orthogonal model ( $dq$ ), the total magnetic flux of the asynchronous machine is calculated. The  $dq$  system is used to study the instantaneous values of the stator and rotor. By transforming the magnetic flux variation equation from the (a, b, c) coordinate system to the ( $\alpha$ ,  $\beta$ , 0) polar coordinate system, the following operations are performed to obtain the stator and rotor equilibrium equations:[5]

$$\begin{bmatrix} \Phi_{as} \\ \Phi_{bs} \\ \Phi_{0s} \end{bmatrix} = \sqrt{\frac{2}{3}} \begin{bmatrix} 1 & -1/2 & -1/2 \\ 0 & \sqrt{3}/2 & -\sqrt{3}/2 \\ \sqrt{2}/2 & \sqrt{2}/2 & \sqrt{2}/2 \end{bmatrix} \cdot \begin{bmatrix} \Phi_{as} \\ \Phi_{bs} \\ \Phi_{cs} \end{bmatrix}, \quad (1)$$

where  $\Phi_{as}$ ,  $\Phi_{bs}$ ,  $\Phi_{cs}$ ,  $\Phi_{\beta s}$  are the components of the stator magnetic flux in the  $\alpha$  and  $\beta$  polar coordinate axes, respectively;  $\Phi_{as}$ ,  $\Phi_{bs}$ ,  $\Phi_{cs}$  are the magnetic flux linkages of the A, B, and C phases in the phase coordinate system. By grouping the first expression, the following set of equations is derived:

$$\left. \begin{aligned} \frac{d\Phi_{as}}{dt} + f_s \Phi_{as} &= u_{as} + f_{\delta s} (\Phi_{ar} \cos \theta_R - \Phi_{\beta r} \sin \theta_R) \\ \frac{d\Phi_{\beta s}}{dt} + f_s \Phi_{\beta s} &= u_{\beta s} + f_{\delta s} (\Phi_{ar} \sin \theta_R + \Phi_{\beta r} \cos \theta_R) \\ \frac{d\Phi_{ar}}{dt} + f_s \Phi_{\beta r} &= f_{\delta r} (\Phi_{as} \cos \theta_R + \Phi_{\beta s} \sin \theta_R) \\ \frac{d\Phi_{\beta r}}{dt} + f_r \Phi_{\beta r} &= f_{\delta r} (-\Phi_{as} \sin \theta_R + \Phi_{\beta s} \cos \theta_R) \end{aligned} \right\} \quad (2)$$

Here,  $\Phi_{ar}$ ,  $\Phi_{\beta r}$  are the components of the rotor magnetic flux in the  $\alpha$  and  $\beta$  polar coordinate axes;  $\theta_R$  is the angle between the magnetic fluxes generated in the stator and rotor;  $\omega_R$  is the rotor angular velocity;  $f_s$  is the frequency generated in the stator winding;  $u_{as}$  is the stator voltage component in the  $\alpha$ -axis;  $f_{\delta s}$  represent the frequency components affecting the stator and rotor through the air gap; corresponds to the zero-sequence component in the polar coordinate system [6-7]. These equations are combined with the motion equation and the working form of the equation system (4 electrical circuits and 1 motion equation):

$$\left. \begin{aligned} \bar{\Phi}_{as}(\bar{s} + f_s) &= \bar{u}_{as} + f_{\delta s} (\bar{\Phi}_{ar} \cos \theta_R + \bar{\Phi}_{\beta r} \sin \theta_R) \\ \bar{\Phi}_{\beta s}(\bar{s} + f_s) &= \bar{u}_{\beta s} + f_{\delta s} (\bar{\Phi}_{ar} \sin \theta_R + \bar{\Phi}_{\beta r} \cos \theta_R) \\ \bar{\Phi}_{ar}(\bar{s} + f_r) &= f_{\sigma r} (\bar{\Phi}_{\beta s} \sin \theta_R + \bar{\Phi}_{as} \cos \theta_R) \\ \bar{\Phi}_{\beta r}(\bar{s} + f_r) &= f_{\sigma r} (-\bar{\Phi}_{as} \sin \theta_R + \bar{\Phi}_{\beta s} \cos \theta_R) \\ \frac{d\theta_R}{dt} &= \dot{\theta}_R = \omega_R \end{aligned} \right\} \quad (3)$$

Equation (3) is simplified under the following conditions: For the two-phase model of the total magnetic flux, components correspond to the polar coordinate system as follows for the rotor (x and y axes)  $\Phi_{xr}$ ,  $\Phi_{yr}$  and for the stator  $\Phi_{xs}$ ,  $\Phi_{ys}$ . Under these conditions, the following expressions hold:

$$\left. \begin{aligned} \Phi_{xr} &= \Phi_{ar} \cos \theta_R - \Phi_{\beta r} \sin \theta_R, & \Phi_{yr} &= \Phi_{ar} \sin \theta_R + \Phi_{\beta r} \cos \theta_R, \\ \Phi_{xs} &= \Phi_{as} \cos \theta_R - \Phi_{\beta s} \sin \theta_R, & \Phi_{ys} &= -\Phi_{as} \sin \theta_R + \Phi_{\beta s} \cos \theta_R. \end{aligned} \right\} \quad (4)$$

If the value of the magnetic flux is conditionally taken as  $\Phi_{ar} = \Phi_{\beta r} = \Phi_{as} = \Phi_{\beta s} = 100$  relative units, the variation equation with respect to  $\theta_R$  (with a step size of 5) is represented.

Mathematical model was developed to describe the magnetic field behavior within the motor, accounting for nonlinearities due to core saturation and slotting effects. The model was validated through finite element simulations and experimental results, showing a high degree of correlation. In Figure 2 above, oscilloscopes of the magnetic field in the air gap of the asynchronous motor under normal operating mode obtained from the mathematical model are

presented, and in Figure 3, oscillograms of the magnetic field in the air gap of the asynchronous motor when one phase is disconnected are shown [8].

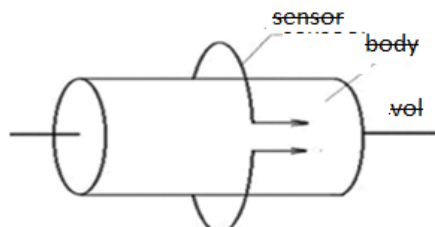


FIGURE 1. Device for measuring the external leakage magnetic field of an asynchronous motor

When the asynchronous motor is connected to the electrical network, an external leakage magnetic field is formed around the housing [9-10]. In this case, the external leakage magnetic field induces an electric driving force in the sensor (measuring conductor). If it is necessary to obtain the oscillogram of the asynchronous motor's external leakage magnetic field 3, the terminals of the sensor (measuring conductor) must be connected to the oscillography vibrator. Figure 3 shows the electrical circuit of this device. According to it, the patented useful model includes a rectangular-shaped measuring frame (sensor) 1 with a diametral pitch and a sinusoidal frame (sensor) 2, whose length is equal to one pole pitch  $\tau$  of the machine. These sensors are placed on the surface of the stator steel core. The device also contains a phase meter 3 and a device 6 for recording the slip angle, which consists of a magnetoelectric instrument 4 and an oscillograph vibrator [11-12].

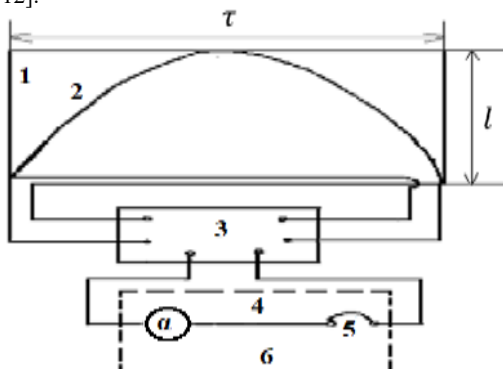


FIGURE 2. Electrical circuit of the device for measuring the phase slip angle of the magnetic field in the air gap of an asynchronous motor

The output terminals of the rectangular coil (sensor) 1 and the sinusoidal coil (sensor) 2 are connected to the vibrator 5 of the oscillograph to measure the phase slip angle between the total electromotive force of the magnetic field formed in the air gap of an asynchronous motor commonly used in industry and the electromotive force of the main harmonic of the magnetic field [13-14]. Figure 3 shows the oscillogram in the steady-state mode of the electromotive force of the magnetic field measured by the rectangular coil 1 and the electromotive force of the main harmonic of the magnetic field measured by the sinusoidal coil (sensor) 2. In steady-state mode, both curves are in phase, so the slip angle  $\alpha$  equals  $0^\circ$  [15].

## RESEARCH RESULTS

The proposed improvements in the magnetic field measurement system for asynchronous motors were experimentally validated through a series of laboratory tests and numerical simulations. The findings confirm the effectiveness of the developed approach in terms of measurement precision, diagnostic reliability, and model performance [16]. When the asynchronous machine operates under load, the magnetic field becomes distorted, leading to deformation in the electromotive force (EMF) waveform measured by the rectangular coil (Sensor 1). As a result,

the EMF corresponding to the fundamental harmonic of the magnetic field measured by the sinusoidal coil (Sensor 2) exhibited a phase shift relative to the EMF measured by Sensor [17-18].

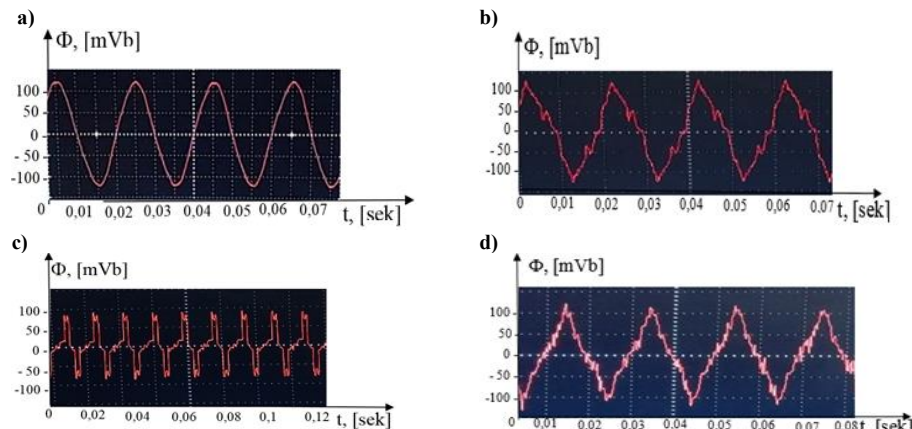


FIGURE 3. a) Oscillogram of the external stray magnetic field of an asynchronous motor with a healthy bearing b) with a faulty bearing c) with one broken rotor bar, d) with vibration present.

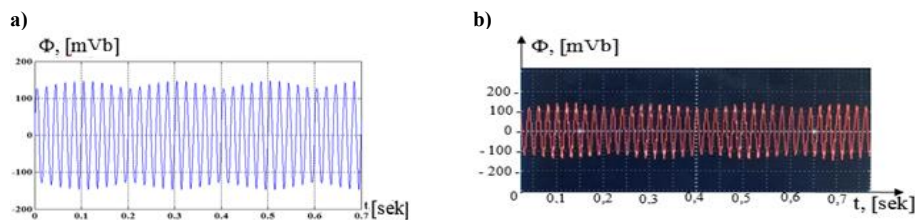


FIGURE 4. Oscillograms of the air gap magnetic field of an asynchronous motor operating with one phase disconnected: (a) mathematical model, (b) obtained from the research object

TABLE 1. Comparison results of air gap magnetic field oscillograms obtained from the mathematical model and the research object of an asynchronous motor operating with one phase open

Type of experiment	The amplitude value of the magnetic field in the air gap is measured in millivolts (mV)	Difference between the results obtained from the mathematical model and the research object
Amplitude value of the air gap magnetic field obtained from the research object (under normal operating conditions)	150	3,44 %
Amplitude value of the air gap magnetic field obtained from the MATLAB Simulink model (under normal operating conditions)	145	
Amplitude value of the air gap magnetic field obtained from the research object (when one phase is interrupted)	150	5,3 %
“Amplitude value of the air gap magnetic field obtained from the Matlab Simulink model (in the case of one phase interrupted)	158	

The amplitude value of the resultant external stray magnetic field sinusoid of the asynchronous motor varies significantly [19-20]. This allows diagnosing the loss of one phase in the asynchronous motor. Below, the oscillograms of the external stray magnetic field obtained from the improved mathematical model and the research object are

compared. According to the comparison results in Table 2, which shows the oscillograms of the external stray magnetic field from the mathematical model and the research object of the asynchronous motor operating with one phase open, the amplitude values of the external stray magnetic field in normal operation and one phase open conditions differ by an average of 6.85% [21-23]. This confirms the adequacy of the mathematical model. The proposed diagnostic method using a device to measure the magnetic field in the air gap of asynchronous motors is important due to its cost-effectiveness and reliability compared to existing diagnostic devices and methods [24-26].

All references in this article have been cited according to the IEEE style, using square brackets, etc., and are listed in the order of their first appearance in the text [27-29]. Equations, figures, and tables have also been referred to using the correct format such as Eq. (1), Fig. 2, and Table 1, in accordance with the referencing requirements. References include relevant academic studies, modeling techniques, hardware designs, and diagnostic methodologies associated with magnetic field analysis and asynchronous motor condition monitoring.

## CONCLUSIONS

This study presented a validated diagnostic framework for asynchronous motors based on advanced magnetic field sensing and robust mathematical modeling. By integrating high-sensitivity Hall-effect sensors with finite element analysis and  $dq$ -axis transformation, the system enabled accurate real-time monitoring of magnetic flux behavior both inside the air gap and around the motor's exterior. Experimental validation showed a close correlation between simulation and real-world data, with average deviations of just 4.37% for internal flux and 6.85% for external field amplitude. These results confirm the model's adequacy and the reliability of the proposed diagnostic method. The enhanced sensing system successfully identified early-stage faults such as rotor bar breakage, stator inter-turn short circuits, and bearing degradation without requiring disassembly or system shutdown. Diagnostic indicators such as waveform distortion and phase angle shifts proved effective in fault detection. Compared to conventional techniques like vibration analysis or motor current signature analysis, this magnetic field-based approach offers a non-invasive, cost-efficient, and sensitive solution suitable for industrial applications and predictive maintenance strategies.

## REFERENCES

1. J. Nizamov, Sh. Ergashov, D. Kurbanbaeva. Phase angle measurement device between the resultable electric drive force and the electric drive force of the main harmonic magnetic field in the air gap of the industrial // AIP Conference Proceedings 3152, 040021, (2024). <https://doi.org/10.1063/5.0218808>
2. J. Nizamov, Sh. Ergashov, O. Berdiyorov, U. Berdiyorov. Device for measuring the resulting magnetic field of the stator winding of asynchronous motor for general industrial application // AIP Conference Proceedings 3152, 050013, (2024). <https://doi.org/10.1063/5.0218809>
3. M. Taniev, U. Mirkhonov, M. Rakhmatova, F. Isakov, S. Ergashov, J. Nizamov Study of the substitution scheme of the parameters of a phase-rotor induction generator // AIP Conference Proceedings 2552, 060010 (2023). <https://doi.org/10.1063/5.0130746>
4. N. Pirmatov, A. Egamov, C. Giyasov, J. Nizamov N. Mamarasulov, U. Berdiyorov. Some aspects of comparing the operational properties of synchronous machines with a conventional and two mutually shifted excitation windings // E3S Web of Conferences <https://doi.org/10.1051/e3sconf/202340103056>
5. K. Alimkhodjaev, M. Mirsaidov, M. Khalikova, J. Nizamov. Transient processes of vibration machines with inertial electric drives // E3S Web of Conferences 2020 <https://doi.org/10.1051/e3sconf/202021601121>
6. G. Mustafakulova, A. Egamov, U. Mirkhonov, J. Nizamov. Calculation and study of the magnetic field of the stator winding of a turbine generator // E3S Web of Conferences 2020 <https://doi.org/10.1051/e3sconf/202021601118>
7. Z. Boilhanov Modeling of asynchronous motor reactive power consumption on the basis of current transducers (2023). <https://doi.org/10.5281/zenodo.10073963>
8. I. Siddikov, A. Malikov, M. Makhsubov, Z. Boikhanov, R. Uzaqov. Study of the static characteristics of the secondary stator voltage converter of the currents of an induction motor. // *American Institute of Physics Conference Series* 2432, 1, 020003, (2022).
9. I. Siddikov, D. Karimjonov, S. A'zamov Uzakov Study on determination of an asynchronous motor's reactive power by the current-to-voltage converter // IOP Conference Series: Earth and Environmental Science, ICECAE-2022. <https://doi.org/10.1088/1755-1315/1142/1/012023>
10. O. Ishnazarov, X. Xaydarov, "Mathematical Analysis of the Impact of External Factors on the Operating Modes of Pump Installations in the Technological Process", *Journal of Academia Open*, 10, 1, 2025,

<https://doi.org/10.21070/acopen.10.2025.10507>.

11. N. Pirmatov, X. Xaydarov, "Investigating the issues of energy saving by means of a mathematical model of transient processes of asynchronous engines in pump units," (in Uzbek), *Journal of Science and innovative development*, vol. 6, no. 5, pp. 63-71, <https://doi.org/10.36522/2181-9637-2023-5-7>
12. J. Nizamov, A. Bekishev, G. Mustafakulova, A. Khalbutayeva, Modeling of reactive power compensation of the electric arc steelmaking furnace DSP-100 UMK at JSC Uzmetkombinat // Aip Conference Proceedings 3331(1) <https://doi.org/0009-0009-3013-9410>
13. O. Toirov, Sh. Azimov, Z. Toirov. Improving the cooling system of reactive power compensation devices used in railway power supply // AIP Conference Proceedings, 3331, 1, 050030, (2025). <https://doi.org/10.1063/5.0305670>
14. O. Toirov, Sh. Azimov, Z. Najmitdinov, M. Sharipov, Z. Toirov. Improvement of the cooling system of reactive power compensating devices used in railway power supply // E3S Web of Conferences, 497, 01015, (2024). <https://doi.org/10.1051/e3sconf/202449701015>
15. D. Jumaeva, O. Toirov, B. Numonov, N. Raxmatullaeva, M. Shamuratova. Obtaining of highly energy-efficient activated carbons based on wood, // E3S Web of Conferences 410, 01018, (2023). <https://doi.org/10.1051/e3sconf/202341001018>
16. D. Jumaeva, O. Toirov, U. Raximov, O. Ergashev, A. Abdyrakhimov. Basic thermodynamic description of adsorption of polar and nonpolar molecules on AOGW, // E3S Web of Conferences 425, 04003 (2023) <https://doi.org/10.1051/e3sconf/202343401020>
17. O. Toirov, M. Taniev, M. Hamdamov, A. Sotiboldiev, Power Losses Of Asynchronous Generators Based On Renewable Energy Sources E3S Web of Conferences, 434, 01020, (2023) <https://doi.org/10.1051/e3sconf/202343401020>
18. O. Toirov, S. Khalikov, Sodikjon Khalikov, F. Sharopov, Studies of reliability indicators of pumping units of machine irrigation on the example of the "Namangan" pumping station, // E3S Web of Conferences 410, 05015, (2023). <https://doi.org/10.1051/e3sconf/202341005015>
19. O. Toirov, D. Bystrov, S. Giyasov, M. Taniev, S. Urokov. Role of Reengineering in Training of Specialists // ACM International Conference Proceeding Series (2020) <https://doi.org/10.1145/3386723.3387868>
20. O. Toirov, V. Ivanova, V. Tsyplkina, D. Jumaeva, D. Abdullaeva, Improvement of the multifilament wire lager for cable production, // E3S Web of Conferences 411, 01041 (2023), <https://doi.org/10.1051/e3sconf/202341101041>
21. O. Toirov, T. Kamalov, U. Mirkhonov, S. Urokov, D. Jumaeva, The mathematical model and a block diagram of a synchronous motor compressor unit with a system of automatic control of the excitation // E3S Web of Conferences, 288, 01083, (2021), <https://doi.org/10.1051/e3sconf/202128801083>
22. O. Toirov, S. Urokov, U. Mirkhonov, H. Afrisal, D. Jumaeva, Experimental study of the control of operating modes of a plate feeder based on a frequency-controlled electric drive, // E3S Web of Conferences, SUSE-2021, 288, 01086 (2021). <https://doi.org/10.1051/e3sconf/202128801086>
23. O. Toirov, S. Khalikov, Diagnostics of pumping units of pumping station of machine water lifting, // E3S Web of Conferences 365, 04013, (2023). <https://doi.org/10.1051/e3sconf/202336504013>
24. O. Toirov, D. Bystrov, M. Gulzoda, Y. Dilfuza, Fuzzy Systems for Computational Linguistics and Natural Language (2020) // ACM International Conference Proceeding Series, <https://doi.org/10.1145/3386723.3387873>
25. O. Toirov, I. Khujaev, J. Jumayev, M. Hamdamov, Modeling of vertical axis wind turbine using Ansys Fluent package program, // E3S Web of Conferences 401, 04040 (2023). <https://doi.org/10.1051/e3sconf/202340104040>
26. O. Toirov, S. Abdi Yonis, Z. Yusupov, A. Habbal, Control Approach Of A Grid Connected Dfig Based Wind Turbine Using Mppt And Pi Controller, // Advances in Electrical and Electronic Engineering, 21, 3, (2023). <https://doi.org/10.15598/aeee.v21i3.5149>
27. D. Jumaeva, A. Abdurakhimov, Kh. Abdurakhimov, N. Rakhmatullaeva, O. Toirov, Energy of adsorption of an adsorbent in solving environmental problems, // E3S Web of Conferences, SUSE-2021, 288, 01082 (2021). <https://doi.org/10.1051/e3sconf/202128801082>
28. O. Toirov, M. Khalikova, D. Jumaeva, S. Kakharov, (2023) Development of a mathematical model of a frequency-controlled electromagnetic vibration motor taking into account the nonlinear dependences of the characteristics of the elements, // E3S Web of Conferences 401, 05089, (2023). <https://doi.org/10.1051/e3sconf/202340105089>
29. S. Khalikov. Analysis of the safety of pumping units of pumping stations of machine water lifting in the function of reliability indicators, // E3S Web of Conferences 365, 04010 (2023), <https://doi.org/10.1051/e3sconf/202336504010>